Downstream signaling induced by several plant Toll/interleukin-1 receptor-containing immune proteins is stable at elevated temperature

Héloïse Demont, Céline Remblière, Raphaël Culerrier, Madeline Sauvaget, Laurent Deslandes, Maud Bernoux

Cell Reports

Downstream signaling induced by several plant Toll/interleukin-1 receptor-containing immune proteins is stable at elevated temperature

Graphical abstract

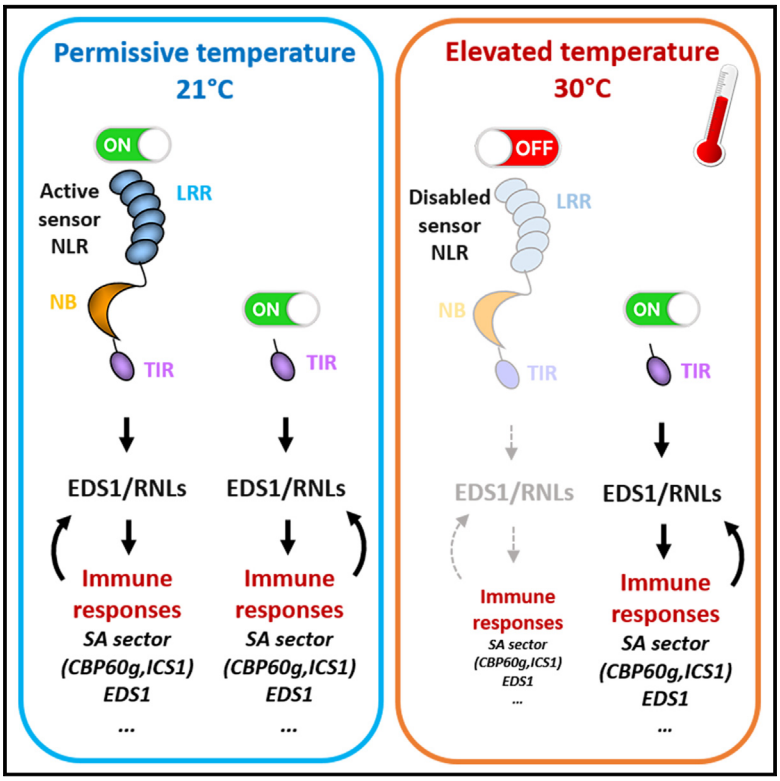

Highlights

- Both TNLs and TIR-only domains activate EDS1/RNL-dependent signaling and the SA sector
- At 30°C, TIR signaling is stable when induced by TIRs only but not by TNLs
- ADR1 and NRG1 RNL members exhibit differential sensitivity to temperature
- Improving NLR resilience to abiotic stresses is key in a changing climate

Authors

Héloïse Demont, Céline Remblière, Raphaël Culerrier, Madeline Sauvaget, Laurent Deslandes, Maud Bernoux

Correspondence

maud.bernoux@inrae.fr

In brief

Demont et al. show that immune signaling induced by Toll/interleukin-1 receptor (TIR) domains, including EDS1 and the SA sector, is maintained at elevated temperatures (30°C), in contrast to signaling induced by full-length TIR-containing NLRs.

Demont et al., 2025, Cell Reports *44*, 115326
March 25, 2025
https://doi.org/10.1016/j.celrep.2025.115326

CellPress

Cell Reports

CellPress
OPEN ACCESS

Report

Downstream signaling induced by several plant Toll/interleukin-1 receptor-containing immune proteins is stable at elevated temperature

Héloïse Demont,[1] Céline Remblière,[1] Raphaël Culerrier,[1] Madeline Sauvaget,[1] Laurent Deslandes,[1] and Maud Bernoux[1,2,*]

[1]Laboratoire des Interactions Plantes-Microbes-Environnement (LIPME), Université de Toulouse, INRAE, CNRS, 31326 Castanet-Tolosan, France

[2]Lead contact

*Correspondence: maud.bernoux@inrae.fr

https://doi.org/10.1016/j.celrep.2025.115326

SUMMARY

Plant immunity and, in particular, immune responses induced by nucleotide-binding leucine-rich repeat receptors (NLRs) are often dampened above the optimal plant's growth range, but the underlying molecular mechanism remains elusive. N-terminal Toll/interleukin-1 receptor (TIR) domains are self-sufficient to trigger immune signaling. We showed that the conditional activation of two well-characterized TIR-containing NLRs (TNLs) or their corresponding TIR domains alone induce the same signaling route at permissive temperature (ENHANCED DISEASE SUSCEPTIBLITY 1 [EDS1]/helper NLRs that display an RPW8-like N-terminal CC_R domain [RNL] requirement and activation of the salicylic acid sector) in *Arabidopsis*. Yet, this signaling pathway is maintained under elevated temperatures (30°C) when induced by TIRs only but not full-length TNLs. This work underlines the need to further study how NLRs are impacted by an increase in temperature, which is particularly important to improve the resilience of plant disease resistance in a warming climate.

INTRODUCTION

A rise in temperature impacts the interaction between plants and microbes, which can result in reduced plant immune responses and increased disease severity.[1–3] Understanding how the plant immune system is impacted by heat stress is crucial to improving the resilience of plant disease resistance in a warming climate.

Plants rely on two major types of immune receptors to fight off pathogens efficiently.[4] At the cell surface, pathogen-recognition receptors (PRRs) recognize microbial- or damaged-associated molecular patterns (MAMPs/DAMPs) and induce pattern-triggered immunity (PTI). Intracellular receptors from the nucleotide-binding (NB) leucine-rich repeat (LRR) receptor (NLR) family recognize microbial effectors that are secreted inside the cell, which induces effector-triggered immunity (ETI). PTI and ETI are closely interconnected and mutually potentiate each other to mount a robust immune response that involves massive transcriptional reprogramming, sometimes culminating in cell death to locally prevent pathogen progression.[5] However, this sophisticated immune network is modulated by temperature changes.[6–14] Importantly, NLR-mediated immune responses are often compromised at elevated temperatures (above 28°C).[2,3] Given the importance of NLRs in crop breeding programs for disease resistance, this is highly concerning in the context of global warming. However, the molecular mechanisms involved remain poorly understood.

Canonical NLRs are modular proteins containing a C-terminal LRR domain, a central NB domain, and an N-terminal signaling domain, which often consists of a Toll/interleukin-1 receptor (TIR) or coiled-coil (CC) domain.[15–18] When TIR- and CC-containing NLRs (TNLs and CNLs, respectively) sense, directly or indirectly, the presence of pathogen effectors, they are qualified as sensor NLRs. A small subclade of NLRs act downstream of sensor NLRs to transduce immune signaling and are therefore called helper NLRs.[19] Helper NLRs that display an RPW8-like N-terminal CC_R domain (RNLs) play a central role in the plant immune system, as they are required for immune signaling induced by multiple sensor NLRs and PRRs.[20–22]

Major breakthroughs have recently shed light on NLR and TIR functions.[23] Upon effector recognition, activated sensor NLRs form oligomeric structures called resistosomes. This promotes TIR-induced proximity and the induction of TIR NADase enzymatic activity, which is required to activate downstream signaling, including the ENHANCED DISEASE SUSCEPTIBLITY 1 (EDS1) family and RNLs.[24–27] In *Arabidopsis*, EDS1 forms mutually exclusive heterodimers with the other two members of the family, PHYTOALEXIN DEFICIENT 4 (PAD4) or SENESCENCE-ASSOCIATED GENE101 (SAG101).[28] NAD^+-derived small molecules specifically bind to either the EDS1-PAD4 or EDS1-SAG101 complex, which in turn selectively associates with and activates different RNL subgroups, ACTIVATED DISEASE RESISTANCE 1 (ADR1) or N REQUIREMENT GENE 1 (NRG1), respectively.[29–31]

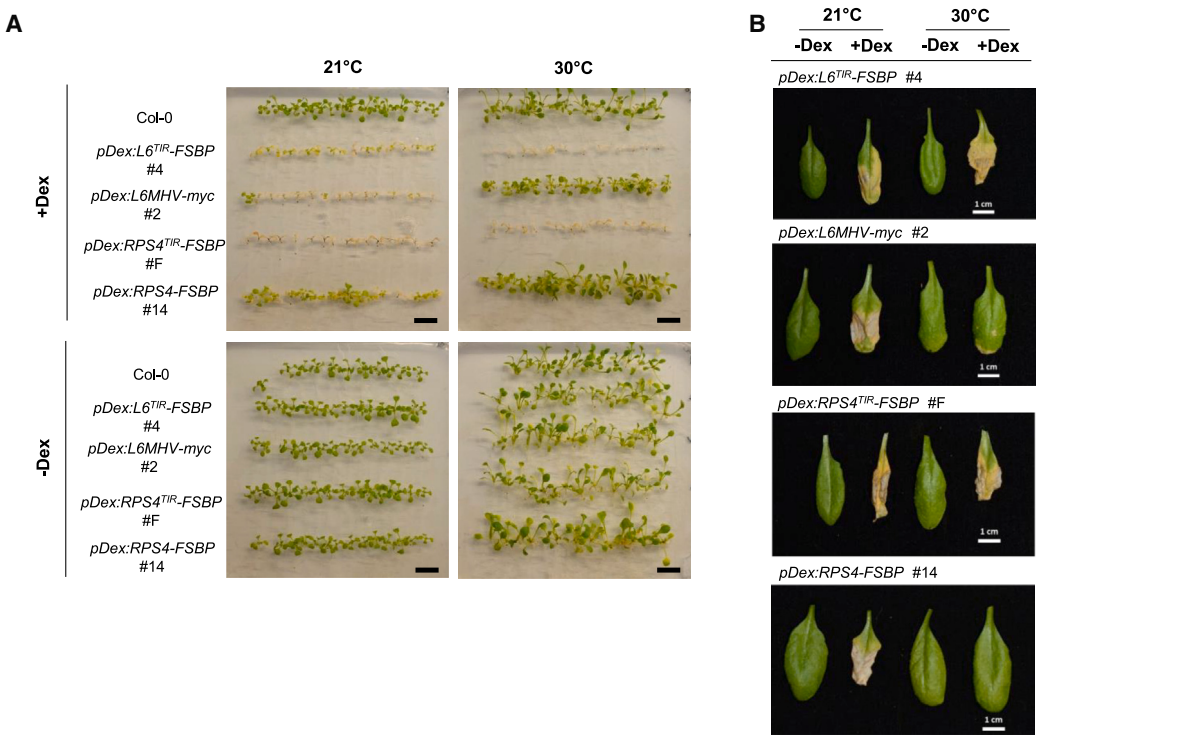

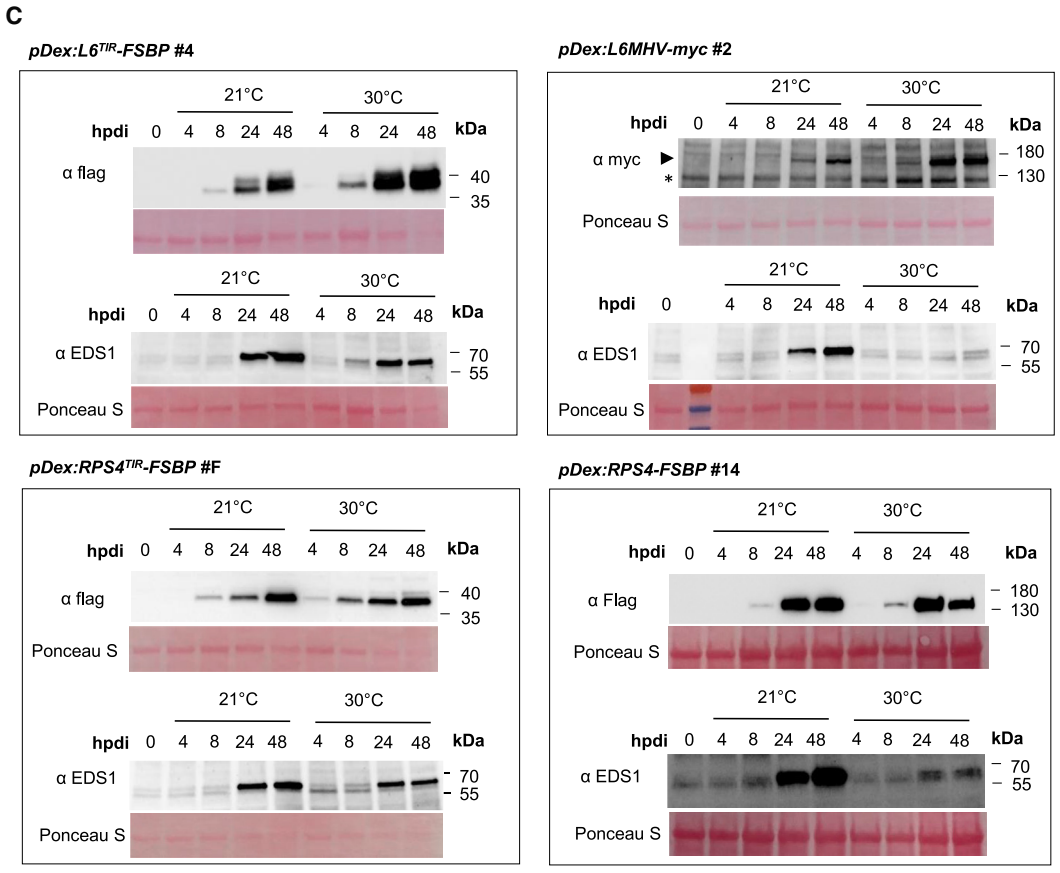

(legend on next page)

Upon activation, RNLs form oligomeric cation-permeable channels targeted to membranes.[32,33] Although RNLs function redundantly, ADR1s seem to predominantly activate transcriptional reprogramming, including genes involved in the salicylic acid (SA) biosynthesis pathway to induce basal immunity, while NRG1s favor the activation of cell death.[21,34] Interestingly, TIR domains also exhibit 2′,3′-cAMP/cGMP synthetase activity, contributing to signaling activation through elusive mechanisms.[29,30,35] SA plays a crucial role in basal immunity and NLR-mediated immune responses.[36,37] However, accumulating evidence features SA as a potential Achilles' heel of plant immunity under elevated temperatures.[7,38] Yet, it is not clear how the SA sector's thermosensitivity impacts NLR activity and signaling, or vice versa. An increase in temperature seems to affect NLR subcellular localization, which could disrupt their function.[12,39] A thermostable variant of the *Arabidopsis* TNL SNC1 maintains its subcellular localization and propagates PAD4-dependent immune signaling, including SA marker PR1, at elevated temperatures, suggesting that increased temperatures might alter receptor functions upstream of induced signaling.[12] However, the underlying mechanisms are not understood.

As signaling units, TIR domains from TNLs can induce autoimmune responses when overexpressed alone *in planta*.[15,17,18,40–42] Hence, they are useful tools to study signaling events downstream of TNL activation, as they bypass effector recognition and complex intradomain interactions or conformational changes during full-length NLR activation. Here, we used inducible *Arabidopsis* transgenic lines expressing TIRs only or corresponding full-length thermosensitive TNLs at permissive (21°C) and non-permissive (30°C) temperatures. We showed that signaling induced by TIRs only but not full-length TNLs is maintained under elevated temperatures, and this includes key actors of TNL signaling, such as EDS1, the SA sector, and RNLs.

RESULTS

Cell death induced by TIR domains alone, but not full-length TNLs, is maintained under elevated temperature

Between 18°C and 22°C, overexpression of the full-length *Arabidopsis* TNL RPS4 and the flax TNL L6MHV autoimmune variant leads to autoimmune responses and cell death in transgenic *Arabidopsis* lines,[9,43,44] and this phenotype is inhibited at 28°C in RPS4-overexpressing lines.[9] To investigate the impact of temperature on TNL-induced immune signaling, we used dexamethasone (Dex)-inducible *Arabidopsis* transgenic lines expressing RPS4 and L6MHV or their corresponding TIR domains alone, RPS4^{TIR} and L6^{TIR}[44] (Table S1), to conditionally activate and monitor autoimmune/cell death symptoms upon induction at permissive (21°C) and elevated (30°C) temperatures.

At permissive temperatures (21°C), *Arabidopsis* seedlings carrying *pDex:L6MHV*, *pDex:L6^{TIR}*, and *pDex:RPS4^{TIR}* constructs developed autoimmune symptoms over 3 to 4 days upon Dex induction to reach seedling death after 7 days[44] (Figure 1A). By contrast, seedlings carrying *pDex:RPS4* showed autoimmune responses but did not die (Figure 1A). Nevertheless, clear cell death was visible on the leaves of 4-week-old plants of all Dex-inducible lines 2–3 days after Dex induction, including lines carrying *pDex:RPS4* (Figure 1B). These results demonstrate that cell death signaling induced by L6^{TIR}, RPS4^{TIR}, and L6MHV can be monitored in both seedling and adult plants, whereas cell death can only be reached in adult plants grown in soil when induced by an overexpression of RPS4 at 21°C. At 30°C, autoimmune and cell death responses in lines carrying *pDex:L6MHV* or *pDex:RPS4* were strongly reduced upon Dex induction (Figures 1A and 1B), supporting that both L6-mediated and RPS4-mediated immunity is compromised at elevated temperatures in our assay. By contrast, lines expressing the corresponding TIR domains alone (L6^{TIR} or RPS4^{TIR}) showed cell death symptoms that were similar to or stronger than what was observed at 21°C (Figure 1A). All protein constructs accumulated in seedlings from 8 h post-Dex induction (hpdi), with increased accumulation over the time monitored (24 and 48 hpdi) (Figure 1C). Protein accumulation kinetics were unchanged or stronger at 30°C compared to 21°C for all constructs (Figure 1C), demonstrating that the inhibition of the cell death phenotype in seedlings carrying *pDex:L6MHV* and *pDex:RPS4* at 30°C is not due to a lack of protein accumulation. An analysis of independent transgenic lines carrying each construct revealed various levels of autoimmune response intensities, from slight stunting to seedling death. Autoimmune phenotype intensity was mostly positively correlated to TNL or TIR protein production levels but not always. Nevertheless, symptoms were always reduced or abolished in *pDex:L6MHV* (*-myc* or *-FSBP* tagged) or *pDex:RPS4* lines at 30°C, despite similar or higher accumulations of L6MHV and RPS4 at 30°C compared to 21°C in both seedlings and adult plants. By contrast, all lines expressing L6^{TIR} and RPS4^{TIR} showed autoimmune responses at 30°C (Figures S1–S4).

Dex-inducible lines expressing the TIR domain of the *Arabidopsis* SNC1 TNL also showed autoimmune symptoms that were similar or stronger at 30°C compared to 21°C (Figure S5), whereas the autoimmune phenotype mediated by a mutation in full-length *SNC1* (*snc1-1*) was reverted at 28°C.[12,45] NLR activity is tightly controlled, notably via intradomain interactions, which could be sensitive to temperature changes. Given their simpler architecture, TIR domains alone are not subjected to such negative regulations, which could explain their heat-stable activity. To test this hypothesis, we generated Dex-inducible lines to conditionally activate naturally occurring, TIR-containing truncated TNLs that were previously described to trigger an immune response when overexpressed, such as TN2 (TIR-NB with no LRR domain) and RBA1 (TIR-only protein with a C-terminal unknown domain).[46,47] Interestingly, induction of

Figure 1. Cell death induced by TIRs only, but not full-length TNLs, is maintained at elevated temperatures in *Arabidopsis*

(A and B) Cell death phenotype of Dex-inducible transgenic seedlings (A) or adult plant leaves (B) carrying *pDex:L6^{TIR}-FSBP*, *pDex:L6MHV-myc*, *pDex:RPS4^{TIR}-FSBP*, or *pDex:RPS4-FSBP* at 21°C and 30°C 7 days after Dex induction. Wild-type Col-0 was used as a negative control. Black scale bars represent 1.5 cm. (C) Immunoblot analysis of L6^{TIR}-FSBP, L6MHV-myc, RPS4^{TIR}-FSBP, RPS4-FSBP, and native EDS1 proteins in transgenic seedlings (as in A) over a time course of 48 h post-Dex induction (hpdi) at 21°C or 30°C. The total protein load is indicated by red Ponceau staining. Background noise is indicated by an asterisk, and the black arrowhead points at L6MHV-myc.

TN2 or RBA1 expression triggered clear autoimmune responses and a cell death phenotype at both temperatures in two independent lines (Figures S6A and S6B). In contrast to TN2, no signal was immunodetected for RBA1 in any of the two selected lines, probably due to RBA1-YFP fusion protein instability (Figure S6C). Surprisingly, RBA1-induced cell death was strongly reduced at 30°C compared to 21°C upon *Pseudomonas fluorescens* (Pf0-1)-mediated delivery of HopBA1 in the Ag-0 natural accession (Figures S7A and S7B). Consistent with previous reports, *RBA1* expression is strongly induced upon infiltration, with Pf0-1 delivering HopBA1 at 21°C in Ag-0, compared to the empty Pf0-1 strain or in the HopBA1-unresponsive Col-0 accession[47,48] (Figure S7C). By contrast, *RBA1* transcripts were reduced to background levels at 30°C upon infiltration with the Pf0-1 HopBA1 strain in Ag-0, similar to the other control conditions (Figure S7C), which may explain why HopBA1-triggered cell death is impaired at 30°C. Altogether, our results demonstrate that the function of canonical TNLs is affected by elevated temperatures, but downstream signaling induced by overexpressed TIR domains is thermostable.

Enhanced expression of *EDS1* and genes involved in the SA sector is maintained under elevated temperature when induced by TIR domains alone but not full-length TNLs

Most TNLs, including RPS4 and L6, depend on an intact catalytic NADase site in their TIR domain, as well as EDS1, to activate immune signaling.[28,44,49] Dex-induced expression of RPS4^{TIR} E88A and L6^{TIR} E135A catalytic mutants did not trigger any visible autoimmune phenotype in *Arabidopsis* seedlings (Figure S8). Furthermore, the RPS4^{TIR}- and L6^{TIR}-triggered cell death phenotype was abrogated in *Arabidopsis eds1-2* mutant background, suggesting that isolated TIRs activate similar signaling routes to sensor TNLs in *Arabidopsis*[42,44] (Figure S9). Interestingly, we showed that native EDS1 protein accumulation was significantly increased in all Dex-inducible lines expressing full-length TNLs (L6MHV and RPS4) or corresponding TIRs alone 24 hpdi at 21°C, in comparison to non-induced seedlings (0 hpdi), and this correlated with the accumulation of inducible protein constructs (Figure 1C). At 30°C, EDS1-enhanced accumulation was maintained upon L6^{TIR} and RPS4^{TIR} induction but not in lines expressing L6MHV and RPS4 (Figures 1C and S6C). Similar results were obtained in lines overexpressing the endogenous truncated TNLs TN2 and RBA1, where EDS1 protein accumulation was enhanced at both 21°C and 30°C (Figure S6C). Consistent with this, *EDS1* expression was upregulated at 21°C upon Dex induction of both full-length TNLs L6MHV and RPS4 or L6^{TIR} and RPS4^{TIR}. However, increased expression of *EDS1* was maintained at 30°C in lines expressing L6^{TIR} and RPS4^{TIR} but not in those expressing L6MHV and RPS4 (Figure 2A). These results further support that temperature elevation disrupts the function and/or properties of full-length TNLs rather than their downstream signaling.

EDS1 promotes SA biosynthesis.[36,37] However, the SA sector seems vulnerable to high temperatures.[38] At 28°C, the expression of major genes involved in SA biosynthesis, such as *CBP60g* and *ICS1*, is dramatically reduced in *Arabidopsis* challenged with virulent bacteria *Pseudomonas syringae* or treated with a synthetic analog of SA (BTH), leading to decreased disease resistance.[38] At 21°C, the expression of *CBP60g* and *ICS1* was upregulated in Dex-inducible lines expressing TNLs or isolated TIRs compared to wild-type Col-0. However, at 30°C, *CBP60g*- and *ICS1*-induced expression was maintained in lines expressing L6^{TIR} and RPS4^{TIR} but not in those expressing L6MHV or RPS4, consistent with the *EDS1* expression profile (Figure 2). Our results show that TNL-mediated signaling is inhibited at 30°C, while signaling induced by TIR domains alone remains stable. Since TIR-mediated signaling can be dose dependent,[48] we verified that this observation was not due to ectopic overexpression of TIR domains. When induced with a lower Dex concentration (0.1 μM), protein accumulation was significantly decreased in seedlings carrying *pDex:L6^{TIR}* and *pDex:RPS4^{TIR}*. Consequently, the associated autoimmune phenotype was reduced (stunting symptoms only) at 21°C, but chlorotic and sometimes necrotic symptoms appeared at a later time after Dex induction at 30°C (Figure S10). Furthermore, *EDS1* and *CBP60g* were significantly induced at both 21°C and 30°C using a low Dex concentration (0.1 μM) compared to non-induced seedlings (Figure S11), supporting that TIR signaling remains stable at 30°C even when TIRs accumulate at low levels. Independent lines accumulating lower levels of L6^{TIR} and RPS4^{TIR} also displayed a clear autoimmune phenotype at 30°C when induced with 10 μM Dex (Figures S1, S2, and S12). When induced with 1 μM Dex, TIR protein accumulation was reduced and closer to that observed in the main transgenic lines *pDex:L6^{TIR}* #4 and *pDex:RPS4^{TIR}* #F when induced with 0.1 μM Dex at 30°C (Figure S12B). Nevertheless, we observed a visible autoimmune phenotype (Figure S12A) and maintained *EDS1* and *CBP60g* upregulation at 30°C (Figure S13), further supporting that TIR signaling is active at both temperatures even when TIRs accumulate at a lower dose. Altogether, these results show that both TNLs and the corresponding TIR domains alone activate the SA sector, but in contrast to full-length NLRs, this sector is maintained at 30°C when induced by TIR domains alone, even at a low dose.

RNLs are required for signaling induced by both TIR domains alone and full-length TNLs

Arabidopsis bares five RNLs that are grouped into ADR1 and NRG1 subfamilies (ADR1, ADR1-L1, and ADR1-L2 and NRG1.1 and NRG1.2, respectively), which translate sensor NLR signaling in an unequally redundant manner, with some functional specificities.[21,34] To test whether thermostable signaling induced by TIRs only requires RNLs, we analyzed Dex-inducible lines carrying RPS4^{TIR}, SNC1^{TIR}, L6^{TIR}, and L6MHV in RNL subgroup mutants (*adr1 triple* [*adr1*, *adr1-L1*, *adr1-L2*], *nrg1 double* [*nrg1.1*, *nrg1.2*], and the *helperless* mutant lacking the five RNLs).[21] In *pDex:RPS4^{TIR}* lines, seedlings were autoimmune in both the wild type and *nrg1 double* mutant. Symptoms were slightly attenuated in *adr1 triple* and fully abolished in the *helperless* mutant (Figure 3A). A similar phenotype was observed in at least two independent lines in each mutant background. Although the autoimmune phenotype intensity induced by RPS4^{TIR} in the *adr1 triple* background seemed to be dose dependent, no phenotype was observed in the *helperless* background even at a high dose (Figure S14), indicating that both NRG1 and ADR1

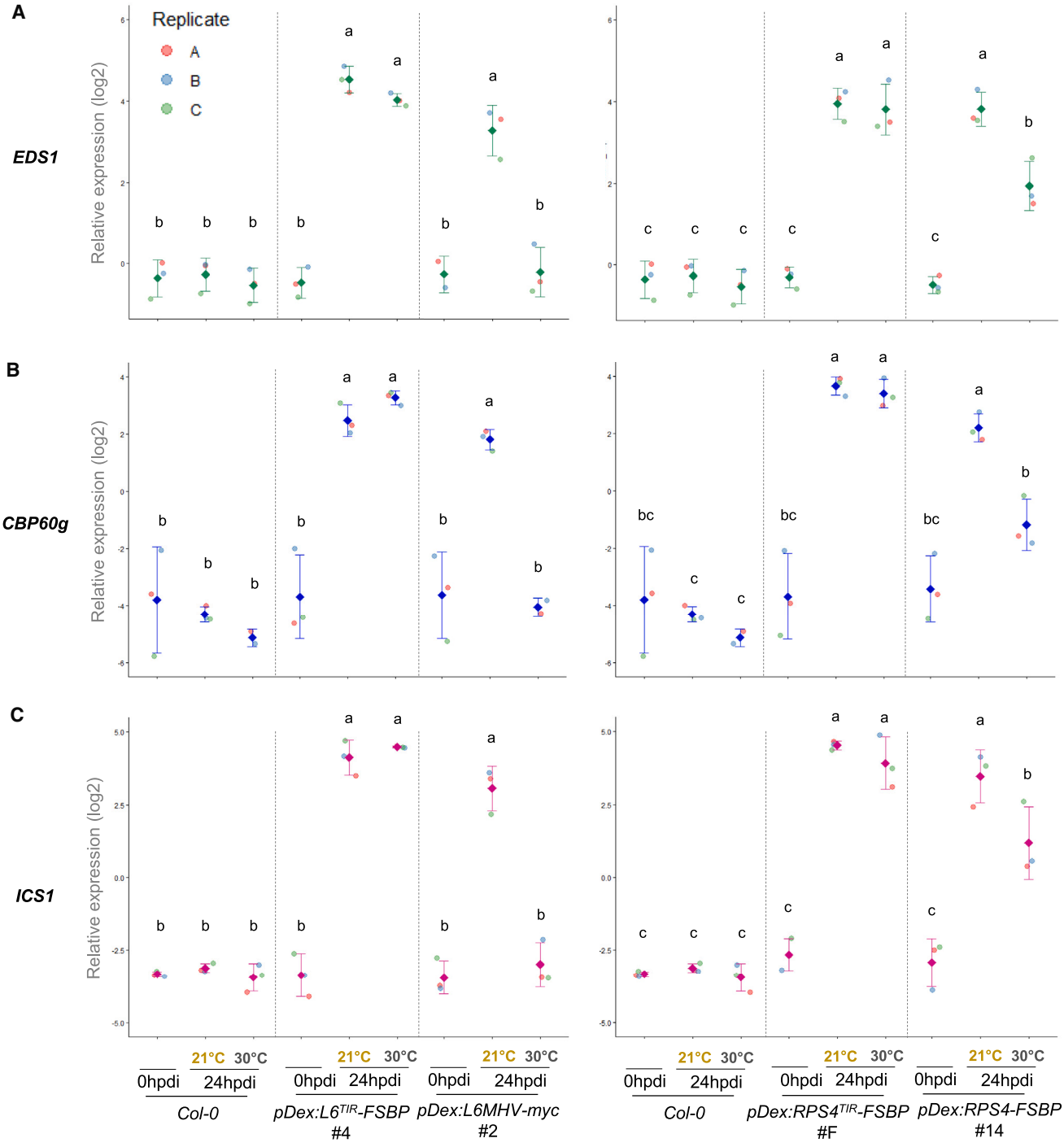

Figure 2. Expression of *EDS1* and genes involved in the SA pathway induced by TIR only, but not full-length TNLs, is maintained at elevated temperature

RT-qPCR analysis of *EDS1* (A), *CBP60g* (B), and *ICS1* (C) transcript levels in wild-type (Col-0) or Dex-inducible transgenic seedlings (as in Figure 1) before (0 hdpi) or 24 hpdi at 21°C or 30°C. Gene expression was normalized with the expression of two housekeeping genes (*At1G13320* and *At5G15710*). Dot plots represent values from three independent biological replicates (colored dots). Statistical differences were assessed with two-way analysis of variance (ANOVA) followed by a Tukey's honestly significant difference (HSD) multiple comparison test. Data points with different letters indicate significant differences ($p < 0.05$).

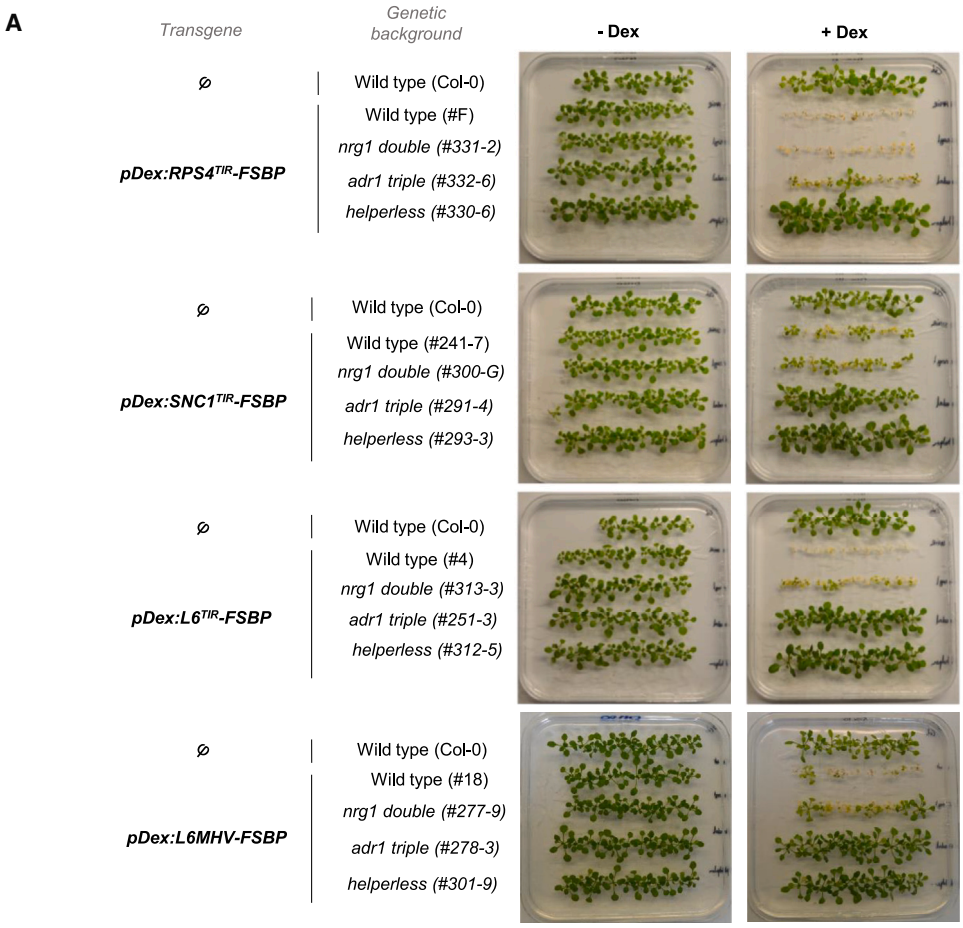

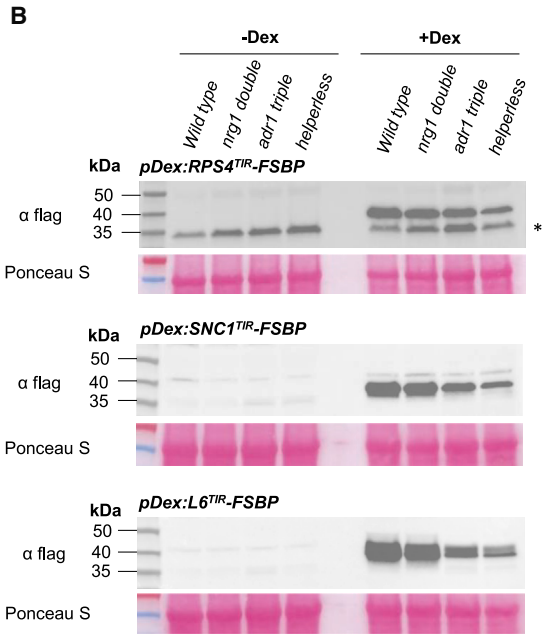

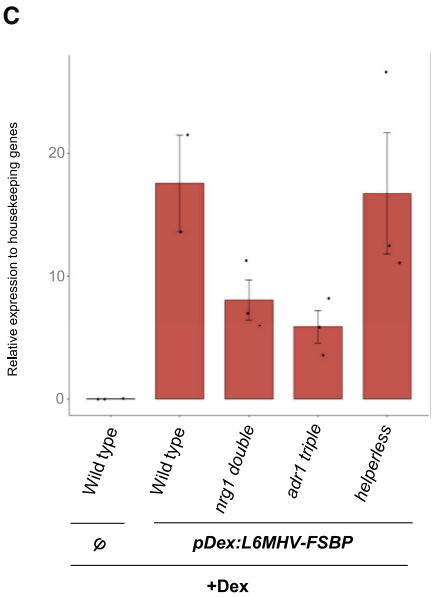

(legend on next page)

families contribute to RPS4^{TIR}-mediated immunity. In lines carrying *pDex:SNC1^{TIR}*, *pDex:L6^{TIR}*, or *pDex:L6MHV*, the autoimmune phenotype was similar or slightly attenuated in *nrg1 double* compared to the wild-type background (Figure 3A). By contrast, very mild or no visible symptoms were visible in the *adr1 triple* and *helperless* mutants, respectively (Figure 3). Similar trends were observed in at least two independent transgenic lines for each construct and each mutant background (Figures S15–S17). We generally observed lower TIR protein accumulation in the *adr1 triple* and *helperless* mutants compared to *nrg1 double* and wild-type backgrounds, especially for L6^{TIR} (Figures 3B, S15, and S16). When using a higher Dex concentration (50 μM), L6^{TIR} protein accumulation was comparable to protein levels in the wild type and *nrg1 double* mutant lines induced at 10 μM Dex. Yet, no visible autoimmune phenotype was visible in *adr1 triple* and the *helperless* mutants, demonstrating that the lack of a cell death phenotype in these genetic backgrounds is not due to lower TIR protein accumulation (Figure S16). L6MHV protein accumulation was too low for immunodetection, so we analyzed transcripts levels and observed some differences in the different mutant backgrounds, with generally lower expression of *L6MHV* in *adr1 triple* and *nrg1 double* compared to the wild-type and *helperless* backgrounds (Figures 3C and S17B). Yet, the induction of *pDex:L6MHV* led to a strong stunting phenotype in the *nrg1 double* mutant, which was comparable to lines in the wild-type background. By contrast, no autoimmune phenotype was observed in the *adr1 triple* and *helperless* mutants (Figures 3A and S17A).

Taken together, these results show that L6^{TIR}, SNC1^{TIR}, RPS4^{TIR}, and L6MHV depend on both ADR1 and NRG1 RNL subgroups to induce signaling, but a lack of NRG1s has a lesser or no impact compared to ADR1s on autoimmune and cell death symptoms induced by SNC1^{TIR}, L6^{TIR}, and L6MHV. Most importantly, our data show that signaling induced by thermostable L6^{TIR} and thermosensitive L6MHV share the same *RNL* genetic requirements.

ADR1 and NRG1 family members show differential temperature sensitivity

RNLs are required for signaling induced by thermostable TIRs only (Figure 3), indicating that RNLs may be resilient to elevated temperatures, unlike sensor TNLs. The ADR1 family mainly contributes to signaling induced by thermosensitive L6MHV and thermostable L6^{TIR}, so we tested whether ADR1-mediated L6^{TIR} signaling was affected at elevated temperatures. *pDex:L6^{TIR}/nrg1 double* lines, carrying functional members of the *ADR1* family, showed clear cell death at both temperatures, demonstrating that ADR1-dependent *L6^{TIR}*-mediated cell death is still effective at 30°C (Figure 4A). To determine whether ADR1s could individually induce thermostable immune signaling, we analyzed the phenotype of the autoimmune line carrying *pADR1-L2:ADR1-L2^{DV}-HA* at 30°C.[50] While this line exhibits constitutive autoimmunity (dwarf, bushy phenotype) at 21°C, with a significantly lower dry weight compared to wild-type Col-0[50] (Figures 4B and 4C), this phenotype was strongly attenuated at 30°C, despite similar levels of ADR1-L2^{DV}-HA accumulation at 21°C or 30°C (Figures 4B–4D). Interestingly, EDS1 accumulation was significantly enhanced in the *pADR1-L2:ADR1-L2^{DV}-HA* line compared to Col-0 at 21°C but was reduced to background levels at 30°C, supporting that signaling induced by ADR1-L2^{DV} is thermosensitive (Figure 4D). Intriguingly, while autoimmune ADR1-L2^{DV} is thermosensitive, *L6^{TIR}* only can activate thermostable ADR1-dependent immunity, suggesting a possible differential temperature sensitivity of ADR1 family members.

ADR1s are mainly required for the autoimmune phenotype induced by L6^{TIR} and SNC1^{TIR}, but both NRG1 and ADR1 families seem to contribute to RPS4^{TIR}-induced signaling (Figure 3A). We investigated whether NRG1 family members are thermostable and found that the autoimmune *pNRG1.1:NRG1.1^{DV}-HA* line[34] displays a strong autoimmune phenotype and enhanced EDS1 protein accumulation at both 21°C and 30°C (Figures 4E–4G), supporting that NRG1.1^{DV}-mediated autoimmunity is resilient to high temperatures. Consistent with this result, Dex-inducible lines carrying *pDex:NRG1.2-FSBP* displayed autoimmune symptoms at 30°C (Figure S18). Overall, these results support that both members of the NRG1 family are thermostable.

Flg22 treatment enhances Dex-induced TNLs and isolated TIR protein accumulation and consequently intensifies immune signaling output

By using Dex-inducible expression, we showed that autoimmune TNLs or TIRs only can activate immune responses and cell death in a PAMP-independent manner (Figure 1). To test whether this response could be potentiated by PTI, we co-treated Dex-induced leaves of adult *Arabidopsis* lines carrying *pDex:L6^{TIR}* or *pDex:L6MHV* with the PTI elicitor flg22 peptide (Figure S19). Two days post-treatment, these lines showed mild chlorosis when treated with Dex only but developed stronger chlorotic symptoms when co-treated with Dex and flg22 (Dex+flg22), and this difference became more evident at 3 days post-treatment, even though cell death intensity was similar 6 days post-treatment. Similar results were observed with at least one independent inducible line carrying *pDex:L6MHV-FSBP* (*#18*) (Figures S19A–S19C). Surprisingly, we repeatedly observed higher protein accumulation of both L6^{TIR} and L6MHV proteins upon Dex+flg22 co-treatment compared to Dex-only treatment. However, the increased accumulation of EDS1 remained steady in both samples, suggesting that Dex+flg22 co-treatment potentiates L6^{TIR}

Figure 3. RNLs are required for signaling induced by both TNLs and TIR-only

(A) Cell death phenotype of Dex-inducible transgenic seedlings carrying *pDex:RPS4^{TIR}-FSBP*, *pDex:SNC1^{TIR}-FSBP*, *pDex:L6^{TIR}-FSBP*, or *pDex:L6MHV-FSBP* in wild-type (WT) or *RNL* mutant backgrounds (*nrg1 double*, *adr1 triple*, or *helperless*) 7 days after Dex induction at 21°C.

(B) Immunoblot analysis of RPS4^{TIR}-FSBP, SNC1^{TIR}-FSBP, and L6^{TIR}-FSBP in WT or *RNL* mutant backgrounds 24 hpdi. The total protein load is indicated by red Ponceau staining. Background noise is indicated by an asterisk.

(C) RT-qPCR analysis of *L6MHV-FSBP* transcript levels in WT or *RNL* mutant backgrounds. Untransformed Col-0 was used as a negative control (A and C). *L6MHV-FSBP* expression was normalized to the expression of two housekeeping genes (*At1G13320* and *At5G15710*). Bar plots represent means ± SEM from two or three independent biological replicates (black dots).

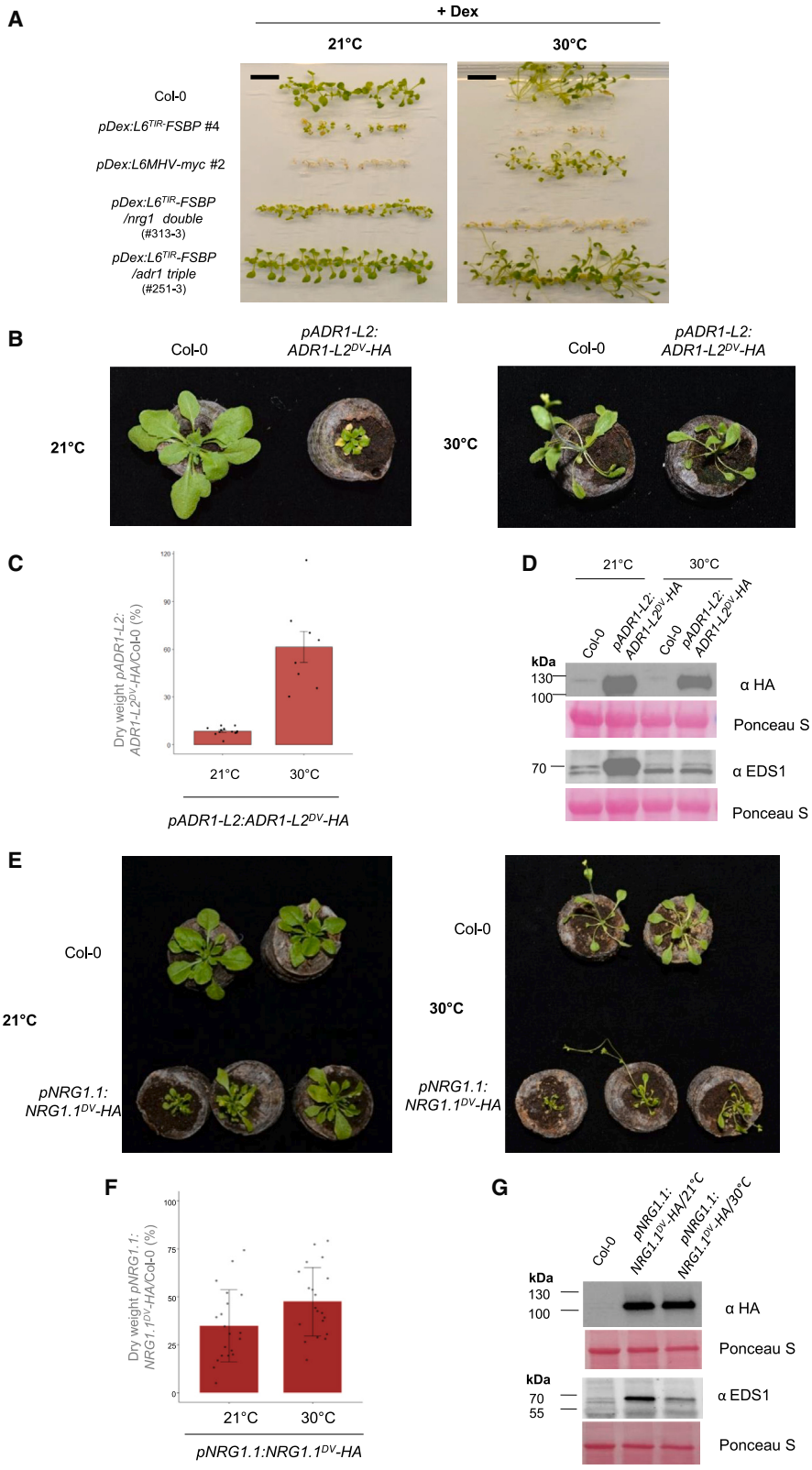

(legend on next page)

and L6MHV protein production but not the increased accumulation of EDS1 (Figure S19D). We obtained similar results with *pDex:RPS4^{TIR}* line #F and two other independent lines (Figure S20). Dex+flg22 co-treatment induced earlier chlorosis/cell death symptoms and enhanced RPS4^{TIR} and RPS4 full-length protein accumulation compared to Dex-only treatment, while EDS1 accumulation remained steady (Figure S20).

These results did not allow us to conclude whether flg22 treatment potentiates TIR signaling or positively impacts the activation of our Dex-inducible system, thus enhancing transcription and protein accumulation, leading to a dose-effect enhanced cell death phenotype. To test this, we used an inducible *Arabidopsis* line carrying a gene construct that is not involved in immunity (*pDex:GFP-MiniTurbo-FLAG*). Similarly to L6^{TIR}, we observed increased levels of GFP-MiniTurbo protein 24 h post-treatment with Dex+flg22 compared to Dex only (Figure S21). This demonstrates that flg22 boosts gene expression of our Dex-inducible system but not native gene expression/protein accumulation, such as EDS1 (Figures S19 and S20), and raises caution in interpreting data on PTI/ETI potentiation when using Dex+flg22 co-treatment. As TIR signaling is dose dependent, the enhanced cell death phenotype observed upon Dex+flg22 co-treatment compared to Dex only may be due to increased protein production by flg22 instead of potentiation of TIR signaling by PTI.

DISCUSSION

NLR activity is often dampened under elevated temperatures, which is concerning in the current climatic context. This observation was previously reported for several TNLs, including *Arabidopsis* SNC1 and RPS4/RRS1 used in this study,[9,10,12] but the underlying molecular mechanisms remain poorly understood. Using Dex-inducible transgenic *Arabidopsis* lines, we showed that immune responses induced by different TIR domains isolated from RPS4, SNC1, and flax L6, are maintained at elevated temperatures even at very low doses, unlike those induced by full-length TNLs, suggesting that a rise of temperature impacts TNL receptor functions but not downstream immune signaling.

Signaling induced by thermostable TIRs only shares the same signaling components as thermosensitive full-length TNLs, which includes EDS1, RNLs, and the SA sector, further supporting that immune responses induced downstream of TNLs, including the SA pathway, are thermostable. Notably, gene expression of master regulators of SA biosynthesis, such as CBP60g and ICS1, is maintained at 30°C in seedlings expressing isolated TIRs only but not full-length NLRs. This result contrasts with earlier studies reporting that elevated temperatures inhibit the SA pathway at its onset by reducing the number of GUANYLATE BINDING PROTEIN-LIKE 3 (GBPL3) defense-activated biomolecular condensates (GDACs). At permissive temperatures, GBPL3 and associated transcriptional coactivators are recruited to the promoter region of *CBP60g* and *SARD1*, which encode master transcription factors regulating the expression of genes involved in SA biosynthesis, such as *ICS1*. Above 28°C, *CBP60g*, *ICS1*, and other SA-related gene expression is strongly reduced in immune-triggered plants due to reduced GDAC numbers.[7,38] Interestingly, overexpressing CBP60g or the EDS1/PAD4 complex is sufficient to recover SA signaling and maintain resistance to virulent and avirulent bacteria at elevated temperatures.[37,38] Hence, the overexpression of immune regulators involved in the SA pathway can bypass the negative impact of elevated temperatures on GDAC formation. Given that the expression of *CBP60g* and *ICS1* is dramatically reduced at 30°C upon the activation of thermosensitive NLRs, but not TIRs only, our results demonstrate that activating downstream TIR signaling is also sufficient to bypass the negative impact of temperature on the SA sector. Hence, it is possible that TNL signaling activates the expression of *CBP60g* in a GDAC-independent manner, resulting in reduced expression in temperature-inactivated TNL- but not thermostable TIR-only-expressing plants.

All TNLs characterized so far require RNLs to induce immune signaling. RNLs function redundantly and contribute differentially to cell death and gene reprogramming.[21,34,51,52] Using *Arabidopsis* lines expressing TIR domains only in different RNL subgroup mutant backgrounds, we showed that TIR-only-mediated signaling depends on RNLs, just like full-length TNLs. L6^{TIR} and SNC1^{TIR} mainly depend on the ADR1 family to translate cell death, which is consistent with the previously reported requirement of ADR1s for an *snc1* autoimmune phenotype.[34] By contrast, both RNL subgroups contribute to RPS4^{TIR}-induced signaling. This slightly differs from previous studies, in which RPS4/RRS1-mediated cell death requires NRG1s, whereas ADR1s support disease resistance and pathogen multiplication restriction.[21] Importantly, our results show that thermostable L6^{TIR} shares the same genetic requirements as the corresponding thermosensitive full-length receptor L6MHV, further supporting that this shared pathway is maintained under elevated temperatures only when induced by TIRs only. Although our data show that RNLs can translate TIR signaling at 30°C, we observed differential temperature sensitivity in RNL subgroup members. The ADR1-L2^{DV}-mediated autoimmune phenotype and associated EDS1 protein accumulation are strongly affected at 30°C. This is consistent with previous studies showing that *ADR1-L2^{DV}*-mediated autoimmunity genetically requires *EDS1*,

Figure 4. Differential temperature sensitivity of ADR1 and NRG1 family members

(A) Cell death phenotype of Dex-inducible transgenic seedlings carrying *pDex:L6^{TIR}* in wild type or *nrg1 double* or *adr1 triple* mutants 7 days after Dex induction at 21°C or 30°C. Untransformed Col-0 was used as a negative control. *pDex:L6MHV-myc* line *#2* was used as a thermosensitive control. The black scale bars represent 1 cm.

(B and E) Representative phenotype of 3-week-old plant carrying *pADR1-L2:ADR1-L2^{DV}-HA* (B) or *pNRG1.1:NRG1.1^{DV}-HA* (E) compared to wild-type Col-0 grown at 21° or 30°C.

(C and F) Percentage of dry weight ratio of *pADR1-L2:ADR1-L2^{DV}-HA* (C) or *pNRG1.1:NRG1.1^{DV}-HA* (F) lines compared to Col-0 at 21°C or 30°C as in (B) and (E), respectively. Bar plots represent the percentage of mean dry weight ratios of plants carrying *pADR1-L2:ADR1-L2^{DV}-HA* or *pNRG1.1:NRG1.1^{DV}-HA*/wild-type Col-0 ± SEM. Individual percentage ratios are represented by black dots ($n > 8$). This experiment was performed twice, with similar results.

(D and G) Immunoblot analysis of ADR1-L2^{DV}-HA (D), NRG1.1^{DV}-HA (G), and EDS1 in 3-week-old transgenics carrying *pADR1-L2:ADR1-L2^{DV}-HA*, *pNRG1.1:NRG1.1^{DV}-HA*, or wild-type Col-0 grown at 21°C or 30°C. The total protein load is indicated by Ponceau red staining.

possibly to positively regulate SA accumulation via a feedback loop,[50,53] which seems to be inhibited at 30°C (this study). Interestingly, the thermostable NRG1.1^{DV}-mediated autoimmune phenotype also triggers the enhanced accumulation of EDS1, which remains stable at 30°C, suggesting that NRG1s may activate a feedback loop that includes *EDS1* upregulation, although NbNRG1s do not genetically require EDS1 to activate cell death in *Nicotiana benthamiana*.[54] The underlying mechanisms will need to be further investigated to fully understand the differential temperature sensitivity of ADR1s and NRG1s. As ADR1-L2^{DV}-mediated autoimmunity signals through TNL *SADR1*,[53] it is possible that SADR1 is thermosensitive like other full-length TNLs, resulting in an attenuated ADR1-L2-mediated autoimmune phenotype. In the wild-type *RNL* background, the presence of other members of the ADR1 family may compensate for ADR1-L2 thermosensitivity by activating SADR1-independent and thermoresilient pathways.

Naturally occurring truncated TNLs lack some of the canonical NLR domains (LRR and/or NB domain) but contain a TIR domain. TIR-only or TIR-NB coding genes are widely represented in the *Arabidopsis* genome, and transcriptional induction of these genes upon immune stimuli indicates that they are broadly involved in plant immunity.[46,47,55,56] Interestingly, we found that two previously described TIR-containing truncated TNLs (RBA1 and TN2) induce thermostable immune signaling when overexpressed, suggesting that thermostable TIR-only signaling may be explained by a simpler architecture compared to full-length TNLs. However, we found that HopBA1-mediated *RBA1* induction is reduced to background levels at 30°C. This prevented us from concluding whether HopBA1-triggered RBA1-dependent cell death is thermostable. Hence, it will be important to thoroughly study the impact of temperature stress on the function of endogenous TIR-containing proteins to determine whether such proteins could protect the immune system under elevated temperatures. Given that NLRs are broadly used in crop breeding programs for disease resistance, this work underlines the need to thoroughly investigate how they are impacted by temperature stress. Canonical sensor TNLs are modular proteins, the activation of which is finely regulated via intra- and interdomain interactions as well as interactions with chaperone proteins.[57–59] Therefore, such regulation may be affected by temperature rise, which in turn may turn off TNL-induced enzymatic activities and downstream signaling.

Several studies have suggested that NLRs could function at the interface between biotic and abiotic stress responses,[60–62] pointing to a role as mediators of growth-defense trade-offs. Hence, it will be important in the future to further investigate how NLR function is modulated by different abiotic stresses.

Limitations of the study

(1) By using inducible transgenic lines expressing autoimmune TNLs or isolated TIRs, this study allowed us to bypass effector recognition to focus on TIR-activated downstream signaling. However, this system revealed limitations, as the signaling output monitored (cell death) is dose dependent.

(2) To deepen our understanding of the impact of temperature stress and the differential requirement of RNL family members for TIR signaling, further analyses on individual RNL members or RNA sequencing (RNA-seq) analyses on *RNL* mutants would be necessary to obtain a full picture of the plant response in these conditions.

(3) Our data were obtained upon a single temperature stress in controlled conditions. It will be important to explore the plant immune response upon combined biotic and abiotic stresses (temperature, drought, and CO_2 levels) to mimic predicted climate change conditions.

RESOURCE AVAILABILITY

Lead contact

Further information and requests for resources and reagents used in this study should be directed to and will be fulfilled by the lead contact, Maud Bernoux (maud.bernoux@inrae.fr).

Materials availability

This study did not generate new unique reagents. All unique plasmids and materials generated in this study are available from the lead contact with a completed materials transfer agreement.

Data and code availability

- Unprocessed photos of immunoblots, seedlings, leaves and plant photos, plant dry weight measurements, and RT-qPCR Ct values obtained in this study have been deposited at Mendeley and are publicly available as of the date of publication. The DOI is listed in the key resources table.
- This paper does not report original code.
- Any additional information required to reanalyze the data reported in this paper is available from the lead contact upon request.

ACKNOWLEDGMENTS

This research was set within the frameworks of the "Laboratoire d'Excellence (LABEX) TULIP" (ANR-10-LABX-41) and the "École Universitaire de Recherche (EUR)" TULIP-GS (ANR-18-EURE-0019). H.D. was supported by a PhD scholarship funded by the French Ministry of National Education and Research. M.B. was supported by a research grant funded by INRAE (Plant Health Department) (PIMS). L.D. was supported by a research grant funded by the Agence Nationale de la Recherche (ANR-18-CE20-0015). We thank Dr. F. El Kasmi (Tubingen University, Germany) for kindly providing *Arabidopsis* mutant lines (*RNLs*) and ADR1 plasmid constructs and for interesting discussions. We also thank Prof. P. Schulze-Lefert (Max Planck Institute for Plant Breeding Research, Cologne, Germany) for providing the Pf0-1 HopBA1 strain and Dr. F. Roux (LIPME, Toulouse, France) for providing the *Arabidopsis* Ag-0 accession.

AUTHOR CONTRIBUTIONS

H.D. and M.B. designed experiments. H.D., R.C., M.S., and M.B. performed experiments. C.R. provided support in generating transgenic plant material. H.D., R.C., M.S., L.D., and M.B. analyzed data. H.D. and M.B. wrote the manuscript. H.D., L.D., and M.B. edited the manuscript.

DECLARATION OF INTERESTS

The authors declare no competing interests.

STAR★METHODS

Detailed methods are provided in the online version of this paper and include the following:

- KEY RESOURCES TABLE
- EXPERIMENTAL MODEL AND STUDY PARTICIPANT DETAILS
  - Bacterial strains and growth conditions

- Plant material and growth conditions
- METHOD DETAILS
  - Plasmid constructions
  - Plant transformation and transgenic lines screening
  - Cell death assays upon dexamethasone induction and/or flg22 treatment
  - Cell death assays upon Pf0-1 infiltration
  - Immunoblot analyses
  - RNA extraction and RT-qPCR analyses
- QUANTIFICATION AND STATISTICAL ANALYSIS

SUPPLEMENTAL INFORMATION

Supplemental information can be found online at https://doi.org/10.1016/j.celrep.2025.115326.

Received: May 5, 2024
Revised: September 19, 2024
Accepted: January 28, 2025

REFERENCES

1. Singh, B.K., Delgado-Baquerizo, M., Egidi, E., Guirado, E., Leach, J.E., Liu, H., and Trivedi, P. (2023). Climate change impacts on plant pathogens, food security and paths forward. Nat. Rev. Microbiol. *21*, 640–656. https://doi.org/10.1038/s41579-023-00900-7.
2. Velásquez, A.C., Castroverde, C.D.M., and He, S.Y. (2018). Plant-Pathogen Warfare under Changing Climate Conditions. Curr. Biol. *28*, R619–R634. https://doi.org/10.1016/j.cub.2018.03.054.
3. Desaint, H., Aoun, N., Deslandes, L., Vailleau, F., Roux, F., and Berthomé, R. (2021). Fight hard or die trying: when plants face pathogens under heat stress. New Phytol. *229*, 712–734. https://doi.org/10.1111/nph.16965.
4. Dodds, P.N., and Rathjen, J.P. (2010). Plant immunity: towards an integrated view of plant-pathogen interactions. Nat. Rev. Genet. *11*, 539–548. https://doi.org/10.1038/nrg2812.
5. Bernoux, M., Zetzsche, H., and Stuttmann, J. (2022). Connecting the dots between cell surface- and intracellular-triggered immune pathways in plants. Curr. Opin. Plant Biol. *69*, 102276. https://doi.org/10.1016/j.pbi.2022.102276.
6. Rasmussen, S., Barah, P., Suarez-Rodriguez, M.C., Bressendorff, S., Friis, P., Costantino, P., Bones, A.M., Nielsen, H.B., and Mundy, J. (2013). Transcriptome responses to combinations of stresses in Arabidopsis. Plant Physiol. *161*, 1783–1794. https://doi.org/10.1104/pp.112.210773.
7. Huot, B., Castroverde, C.D.M., Velásquez, A.C., Hubbard, E., Pulman, J.A., Yao, J., Childs, K.L., Tsuda, K., Montgomery, B.L., and He, S.Y. (2017). Dual impact of elevated temperature on plant defence and bacterial virulence in Arabidopsis. Nat. Commun. *8*, 1808. https://doi.org/10.1038/s41467-017-01674-2.
8. Cheng, C., Gao, X., Feng, B., Sheen, J., Shan, L., and He, P. (2013). Plant immune response to pathogens differs with changing temperatures. Nat. Commun. *4*, 2530. https://doi.org/10.1038/ncomms3530.
9. Heidrich, K., Tsuda, K., Blanvillain-Baufumé, S., Wirthmueller, L., Bautor, J., and Parker, J.E. (2013). Arabidopsis TNL-WRKY domain receptor RRS1 contributes to temperature-conditioned RPS4 auto-immunity. Front. Plant Sci. *4*, 403. https://doi.org/10.3389/fpls.2013.00403.
10. Aoun, N., Tauleigne, L., Lonjon, F., Deslandes, L., Vailleau, F., Roux, F., and Berthomé, R. (2017). Quantitative Disease Resistance under Elevated Temperature: Genetic Basis of New Resistance Mechanisms to. Front. Plant Sci. *8*, 1387. https://doi.org/10.3389/fpls.2017.01387.
11. Negeri, A., Wang, G.F., Benavente, L., Kibiti, C.M., Chaikam, V., Johal, G., and Balint-Kurti, P. (2013). Characterization of temperature and light effects on the defense response phenotypes associated with the maize Rp1-D21 autoactive resistance gene. BMC Plant Biol. *13*, 106. https://doi.org/10.1186/1471-2229-13-106.
12. Zhu, Y., Qian, W., and Hua, J. (2010). Temperature modulates plant defense responses through NB-LRR proteins. PLoS Pathog. *6*, e1000844. https://doi.org/10.1371/journal.ppat.1000844.
13. Whitham, S., McCormick, S., and Baker, B. (1996). The N gene of tobacco confers resistance to tobacco mosaic virus in transgenic tomato. Proc. Natl. Acad. Sci. USA *93*, 8776–8781. https://doi.org/10.1073/pnas.93.16.8776.
14. Jablonska, B., Ammiraju, J.S.S., Bhattarai, K.K., Mantelin, S., Martinez de Ilarduya, O., Roberts, P.A., and Kaloshian, I. (2007). The Mi-9 gene from Solanum arcanum conferring heat-stable resistance to root-knot nematodes is a homolog of Mi-1. Plant Physiol. *143*, 1044–1054. https://doi.org/10.1104/pp.106.089615.
15. Bernoux, M., Ve, T., Williams, S., Warren, C., Hatters, D., Valkov, E., Zhang, X., Ellis, J.G., Kobe, B., and Dodds, P.N. (2011). Structural and functional analysis of a plant resistance protein TIR domain reveals interfaces for self-association, signaling, and autoregulation. Cell Host Microbe *9*, 200–211. https://doi.org/10.1016/j.chom.2011.02.009.
16. Cesari, S., Moore, J., Chen, C., Webb, D., Periyannan, S., Mago, R., Bernoux, M., Lagudah, E.S., and Dodds, P.N. (2016). Cytosolic activation of cell death and stem rust resistance by cereal MLA-family CC-NLR proteins. Proc. Natl. Acad. Sci. USA *113*, 10204–10209. https://doi.org/10.1073/pnas.1605483113.
17. Williams, S.J., Sohn, K.H., Wan, L., Bernoux, M., Sarris, P.F., Segonzac, C., Ve, T., Ma, Y., Saucet, S.B., Ericsson, D.J., et al. (2014). Structural basis for assembly and function of a heterodimeric plant immune receptor. Science *344*, 299–303. https://doi.org/10.1126/science.1247357.
18. Zhang, X., Bernoux, M., Bentham, A.R., Newman, T.E., Ve, T., Casey, L.W., Raaymakers, T.M., Hu, J., Croll, T.I., Schreiber, K.J., et al. (2017). Multiple functional self-association interfaces in plant TIR domains. Proc. Natl. Acad. Sci. USA *114*, E2046–E2052. https://doi.org/10.1073/pnas.1621248114.
19. Contreras, M.P., Lüdke, D., Pai, H., Toghani, A., and Kamoun, S. (2023). NLR receptors in plant immunity: making sense of the alphabet soup. EMBO Rep. *24*, e57495. https://doi.org/10.15252/embr.202357495.
20. Collier, S.M., Hamel, L.P., and Moffett, P. (2011). Cell death mediated by the N-terminal domains of a unique and highly conserved class of NB-LRR pcrotein. Mol. Plant Microbe Interact. *24*, 918–931. https://doi.org/10.1094/mpmi-03-11-0050.
21. Saile, S.C., Jacob, P., Castel, B., Jubic, L.M., Salas-Gonzáles, I., Bäcker, M., Jones, J.D.G., Dangl, J.L., and El Kasmi, F. (2020). Two unequally redundant "helper" immune receptor families mediate Arabidopsis thaliana intracellular "sensor" immune receptor functions. PLoS Biol. *18*, e3000783. https://doi.org/10.1371/journal.pbio.3000783.
22. Pruitt, R.N., Locci, F., Wanke, F., Zhang, L., Saile, S.C., Joe, A., Karelina, D., Hua, C., Fröhlich, K., Wan, W.L., et al. (2021). The EDS1-PAD4-ADR1 node mediates Arabidopsis pattern-triggered immunity. Nature *598*, 495–499. https://doi.org/10.1038/s41586-021-03829-0.
23. Maruta, N., Burdett, H., Lim, B.Y.J., Hu, X., Desa, S., Manik, M.K., and Kobe, B. (2022). Structural basis of NLR activation and innate immune signalling in plants. Immunogenetics *74*, 5–26. https://doi.org/10.1007/s00251-021-01242-5.
24. Horsefield, S., Burdett, H., Zhang, X., Manik, M.K., Shi, Y., Chen, J., Qi, T., Gilley, J., Lai, J.S., Rank, M.X., et al. (2019). NAD + cleavage activity by animal and plant TIR domains in cell death pathways. Science *365*, 793–799. https://doi.org/10.1126/science.aax1911.
25. Wan, L., Essuman, K., Anderson, R.G., Sasaki, Y., Monteiro, F., Chung, E.H., Osborne Nishimura, E., DiAntonio, A., Milbrandt, J., Dangl, J.L., and Nishimura, M.T. (2019). TIR domains of plant immune receptors are NAD. Science *365*, 799–803. https://doi.org/10.1126/science.aax1771.
26. Martin, R., Qi, T., Zhang, H., Liu, F., King, M., Toth, C., Nogales, E., and Staskawicz, B.J. (2020). Structure of the activated ROQ1 resistosome

directly recognizing the pathogen effector XopQ. Science *370*, eabd9993. https://doi.org/10.1126/science.abd9993.

27. Ma, S., Lapin, D., Liu, L., Sun, Y., Song, W., Zhang, X., Logemann, E., Yu, D., Wang, J., Jirschitzka, J., et al. (2020). Direct pathogen-induced assembly of an NLR immune receptor complex to form a holoenzyme. Science *370*, eabe3069. https://doi.org/10.1126/science.abe3069.
28. Lapin, D., Bhandari, D.D., and Parker, J.E. (2020). Origins and Immunity Networking Functions of EDS1 Family Proteins. Annu. Rev. Phytopathol. *58*, 253–276. https://doi.org/10.1146/annurev-phyto-010820-012840.
29. Huang, S., Jia, A., Song, W., Hessler, G., Meng, Y., Sun, Y., Xu, L., Laessle, H., Jirschitzka, J., Ma, S., et al. (2022). Identification and receptor mechanism of TIR-catalyzed small molecules in plant immunity. Science *377*, eabq3297. https://doi.org/10.1126/science.abq3297.
30. Jia, A., Huang, S., Song, W., Wang, J., Meng, Y., Sun, Y., Xu, L., Laessle, H., Jirschitzka, J., Hou, J., et al. (2022). TIR-catalyzed ADP-ribosylation reactions produce signaling molecules for plant immunity. Science *377*, eabq8180. https://doi.org/10.1126/science.abq8180.
31. Sun, X., Lapin, D., Feehan, J.M., Stolze, S.C., Kramer, K., Dongus, J.A., Rzemieniewski, J., Blanvillain-Baufumé, S., Harzen, A., Bautor, J., et al. (2021). Pathogen effector recognition-dependent association of NRG1 with EDS1 and SAG101 in TNL receptor immunity. Nat. Commun. *12*, 3335. https://doi.org/10.1038/s41467-021-23614-x.
32. Jacob, P., Kim, N.H., Wu, F., El-Kasmi, F., Chi, Y., Walton, W.G., Furzer, O.J., Lietzan, A.D., Sunil, S., Kempthorn, K., et al. (2021). Plant "helper" immune receptors are Ca. Science *373*, 420–425. https://doi.org/10.1126/science.abg7917.
33. Feehan, J.M., Wang, J., Sun, X., Choi, J., Ahn, H.K., Ngou, B.P.M., Parker, J.E., and Jones, J.D.G. (2023). Oligomerization of a plant helper NLR requires cell-surface and intracellular immune receptor activation. Proc. Natl. Acad. Sci. USA *120*, e2210406120. https://doi.org/10.1073/pnas.2210406120.
34. Wu, Z., Li, M., Dong, O.X., Xia, S., Liang, W., Bao, Y., Wasteneys, G., and Li, X. (2019). Differential regulation of TNL-mediated immune signaling by redundant helper CNLs. New Phytol. *222*, 938–953. https://doi.org/10.1111/nph.15665.
35. Yu, D., Song, W., Tan, E.Y.J., Liu, L., Cao, Y., Jirschitzka, J., Li, E., Logemann, E., Xu, C., Huang, S., et al. (2022). TIR domains of plant immune receptors are 2',3'-cAMP/cGMP synthetases mediating cell death. Cell *185*, 2370–2386.e18. https://doi.org/10.1016/j.cell.2022.04.032.
36. Wiermer, M., Feys, B.J., and Parker, J.E. (2005). Plant immunity: the EDS1 regulatory node. Curr. Opin. Plant Biol. *8*, 383–389. https://doi.org/10.1016/j.pbi.2005.05.010.
37. Cui, H., Gobbato, E., Kracher, B., Qiu, J., Bautor, J., and Parker, J.E. (2017). A core function of EDS1 with PAD4 is to protect the salicylic acid defense sector in Arabidopsis immunity. New Phytol. *213*, 1802–1817. https://doi.org/10.1111/nph.14302.
38. Kim, J.H., Castroverde, C.D.M., Huang, S., Li, C., Hilleary, R., Seroka, A., Sohrabi, R., Medina-Yerena, D., Huot, B., Wang, J., et al. (2022). Increasing the resilience of plant immunity to a warming climate. Nature *607*, 339–344. https://doi.org/10.1038/s41586-022-04902-y.
39. Mang, H.G., Qian, W., Zhu, Y., Qian, J., Kang, H.G., Klessig, D.F., and Hua, J. (2012). Abscisic acid deficiency antagonizes high-temperature inhibition of disease resistance through enhancing nuclear accumulation of resistance proteins SNC1 and RPS4 in Arabidopsis. Plant Cell *24*, 1271–1284. https://doi.org/10.1105/tpc.112.096198.
40. Krasileva, K.V., Dahlbeck, D., and Staskawicz, B.J. (2010). Activation of an Arabidopsis resistance protein is specified by the in planta association of its leucine-rich repeat domain with the cognate oomycete effector. Plant Cell *22*, 2444–2458. https://doi.org/10.1105/tpc.110.075358.
41. Williams, S.J., Yln, L., Foley, G., Casey, L.W., Outram, M.A., Ericsson, D.J., Lu, J., Boden, M., Dry, I.B., and Kobe, B. (2016). Structure and function of the TIR domain from the grape NLR protein RPV1. Front. Plant Sci. *7*, 1850. https://doi.org/10.3389/fpls.2016.01850.
42. Swiderski, M.R., Birker, D., and Jones, J.D.G. (2009). The TIR domain of TIR-NB-LRR resistance proteins is a signaling domain involved in cell death induction. Mol. Plant Microbe Interact. *22*, 157–165.
43. Howles, P., Lawrence, G., Finnegan, J., McFadden, H., Ayliffe, M., Dodds, P., and Ellis, J. (2005). Autoactive alleles of the flax L6 rust resistance gene induce non-race-specific rust resistance associated with the hypersensitive response. Mol. Plant Microbe Interact. *18*, 570–582.
44. Bernoux, M., Chen, J., Zhang, X., Newell, K., Hu, J., Deslandes, L., and Dodds, P. (2023). Subcellular localization requirements and specificities for plant immune receptor Toll-interleukin-1 receptor signaling. Plant J. *114*, 1319–1337. https://doi.org/10.1111/tpj.16195.
45. Yang, S., and Hua, J. (2004). A haplotype-specific Resistance gene regulated by BONZAI1 mediates temperature-dependent growth control in Arabidopsis. Plant Cell *16*, 1060–1071. https://doi.org/10.1105/tpc.020479.
46. Nandety, R.S., Caplan, J.L., Cavanaugh, K., Perroud, B., Wroblewski, T., Michelmore, R.W., and Meyers, B.C. (2013). The role of TIR-NBS and TIR-X proteins in plant basal defense responses. Plant Physiol. *162*, 1459–1472. https://doi.org/10.1104/pp.113.219162.
47. Nishimura, M.T., Anderson, R.G., Cherkis, K.A., Law, T.F., Liu, Q.L., Machius, M., Nimchuk, Z.L., Yang, L., Chung, E.H., El Kasmi, F., et al. (2017). TIR-only protein RBA1 recognizes a pathogen effector to regulate cell death in Arabidopsis. Proc. Natl. Acad. Sci. USA *114*, E2053–E2062. https://doi.org/10.1073/pnas.1620973114.
48. Song, W., Liu, L., Yu, D., Bernardy, H., Jirschitzka, J., Huang, S., Jia, A., Jemielniak, W., Acker, J., Laessle, H., et al. (2024). Substrate-induced condensation activates plant TIR domain proteins. Nature *627*, 847–853. https://doi.org/10.1038/s41586-024-07183-9.
49. Li, X., Clarke, J.D., Zhang, Y., and Dong, X. (2001). Activation of an EDS1-mediated R-gene pathway in the snc1 mutant leads to constitutive, NPR1-independent pathogen resistance. Mol. Plant Microbe Interact. *14*, 1131–1139. https://doi.org/10.1094/MPMI.2001.14.10.1131.
50. Roberts, M., Tang, S., Stallmann, A., Dangl, J.L., and Bonardi, V. (2013). Genetic requirements for signaling from an autoactive plant NB-LRR intracellular innate immune receptor. PLoS Genet. *9*, e1003465. https://doi.org/10.1371/journal.pgen.1003465.
51. Dong, O.X., Tong, M., Bonardi, V., El Kasmi, F., Woloshen, V., Wünsch, L.K., Dangl, J.L., and Li, X. (2016). TNL-mediated immunity in Arabidopsis requires complex regulation of the redundant ADR1 gene family. New Phytol. *210*, 960–973. https://doi.org/10.1111/nph.13821.
52. Castel, B., Ngou, P.M., Cevik, V., Redkar, A., Kim, D.S., Yang, Y., Ding, P., and Jones, J.D.G. (2019). Diverse NLR immune receptors activate defence via the RPW8-NLR NRG1. New Phytol. *222*, 966–980. https://doi.org/10.1111/nph.15659.
53. Jacob, P., Hige, J., Song, L., Bayless, A., Russ, D., Bonardi, V., El Kasmi, F., Wünsch, L., Yang, Y., Fitzpatrick, C.R., et al. (2023). Broader functions of TIR domains in Arabidopsis immunity. Proc. Natl. Acad. Sci. USA *120*, e2220921120. https://doi.org/10.1073/pnas.2220921120.
54. Qi, T., Seong, K., Thomazella, D.P.T., Kim, J.R., Pham, J., Seo, E., Cho, M.J., Schultink, A., and Staskawicz, B.J. (2018). NRG1 functions downstream of EDS1 to regulate TIR-NLR-mediated plant immunity. Proc. Natl. Acad. Sci. USA *115*, E10979–E10987. https://doi.org/10.1073/pnas.1814856115.
55. Meyers, B.C., Morgante, M., and Michelmore, R.W. (2002). TIR-X and TIR-NBS proteins: two new families related to disease resistance TIR-NBS-LRR proteins encoded in Arabidopsis and other plant genomes. Plant J. *32*, 77–92.
56. Liang, W., van Wersch, S., Tong, M., and Li, X. (2019). TIR-NB-LRR immune receptor SOC3 pairs with truncated TIR-NB protein CHS1 or TN2 to monitor the homeostasis of E3 ligase SAUL1. New Phytol. *221*, 2054–2066. https://doi.org/10.1111/nph.15534.
57. Bernoux, M., Burdett, H., Williams, S.J., Zhang, X., Chen, C., Newell, K., Lawrence, G.J., Kobe, B., Ellis, J.G., Anderson, P.A., and Dodds, P.N. (2016). Comparative Analysis of the Flax Immune Receptors L6 and L7

Suggests an Equilibrium-Based Switch Activation Model. Plant Cell *28*, 146–159. https://doi.org/10.1105/tpc.15.00303.

58. Ravensdale, M., Bernoux, M., Ve, T., Kobe, B., Thrall, P.H., Ellis, J.G., and Dodds, P.N. (2012). Intramolecular interaction influences binding of the Flax L5 and L6 resistance proteins to their AvrL567 ligands. PLoS Pathog. *8*, e1003004. https://doi.org/10.1371/journal.ppat.1003004.
59. Shirasu, K. (2009). The HSP90-SGT1 chaperone complex for NLR immune sensors. Annu. Rev. Plant Biol. *60*, 139–164. https://doi.org/10.1146/annurev.arplant.59.032607.092906.
60. Ariga, H., Katori, T., Tsuchimatsu, T., Hirase, T., Tajima, Y., Parker, J.E., Alcázar, R., Koornneef, M., Hoekenga, O., Lipka, A.E., et al. (2017). NLR locus-mediated trade-off between abiotic and biotic stress adaptation in Arabidopsis. Nat. Plants *3*, 17072. https://doi.org/10.1038/nplants.2017.72.
61. Chen, K., Gao, J., Sun, S., Zhang, Z., Yu, B., Li, J., Xie, C., Li, G., Wang, P., Song, C.P., et al. (2020). BONZAI Proteins Control Global Osmotic Stress Responses in Plants. Curr. Biol. *30*, 4815–4825.e4. https://doi.org/10.1016/j.cub.2020.09.016.
62. Zbierzak, A.M., Porfirova, S., Griebel, T., Melzer, M., Parker, J.E., and Dörmann, P. (2013). A TIR-NBS protein encoded by Arabidopsis Chilling Sensitive 1 (CHS1) limits chloroplast damage and cell death at low temperature. Plant J. *75*, 539–552. https://doi.org/10.1111/tpj.12219.
63. Craft, J., Samalova, M., Baroux, C., Townley, H., Martinez, A., Jepson, I., Tsiantis, M., and Moore, I. (2005). New pOp/LhG4 vectors for stringent glucocorticoid-dependent transgene expression in Arabidopsis. Plant J. *41*, 899–918. https://doi.org/10.1111/j.1365-313X.2005.02342.x.
64. Wielopolska, A., Townley, H., Moore, I., Waterhouse, P., and Helliwell, C. (2005). A high-throughput inducible RNAi vector for plants. Plant Biotechnol. J. *3*, 583–590. https://doi.org/10.1111/j.1467-7652.2005.00149.x.
65. Bernoux, M., Timmers, T., Jauneau, A., Brière, C., de Wit, P.J.G.M., Marco, Y., and Deslandes, L. (2008). RD19, an Arabidopsis cysteine protease required for RRS1-R-mediated resistance, is relocalized to the nucleus by the Ralstonia solanacearum PopP2 effector. Plant Cell *20*, 2252–2264.
66. Mair, A., Xu, S.L., Branon, T.C., Ting, A.Y., and Bergmann, D.C. (2019). Proximity labeling of protein complexes and cell-type-specific organellar proteomes in. Elife *8*, e47864. https://doi.org/10.7554/eLife.47864.
67. Bartsch, M., Gobbato, E., Bednarek, P., Debey, S., Schultze, J.L., Bautor, J., and Parker, J.E. (2006). Salicylic acid-independent ENHANCED DISEASE SUSCEPTIBILITY1 signaling in Arabidopsis immunity and cell death is regulated by the monooxygenase FMO1 and the Nudix hydrolase NUDT7. Plant Cell *18*, 1038–1051. https://doi.org/10.1105/tpc.105.039982.

STAR★METHODS

KEY RESOURCES TABLE

REAGENT or RESOURCE	SOURCE	IDENTIFIER
Antibodies		
anti-HA-peroxidase, High affinity	Roche	Cat#12013819001; RRID: AB_390917
anti-FLAG-M2-peroxidase	Sigma-Aldrich	Cat#SAB4200119; RRID: AB_3675946
anti-GFP from mouse IgG1k (clones 7.1 and 13.1)	Roche	Cat#11814460001; RRID: AB_390913
anti-*c*-myc-peroxidase	Roche	Cat#11814150001; RRID: AB_390910
anti-EDS1	Jane Parker (MPI, Cologne)	N/A
goat anti-rabbit-HRP IgG (H + L)-HRP conjugate	Bio-Rad	Cat#170-6515; RRID: AB_11125142
Chemicals, peptides		
Dexamethasone	Sigma-Aldrich	Cat#D4902
Z-Leu-Leu-Leu-al (MG132)	Sigma-Aldrich	Cat#C2211
Protease inhibitor cocktail	Sigma-Aldrich	Cat#P9599
flg22 peptide	CASLO laboratory	Lot No: P121009-01-01
Gentamicin sulfate	Duchefa Biochemie	Cat#1405-41-0
Carbenicillin disodium	Duchefa Biochemie	Cat#4800-94-6
Spectinomycin pentahydrate	Duchefa Biochemie	Cat#22189-32-8
Chloramphenicol	Duchefa Biochemie	Cat#56-75-7
Kanamycin sulfate monohydrate	Duchefa Biochemie	Cat#25389-94-0
Tetracycline hydrochloride	Sigma-Aldrich	Cat#T7660
3′,5′-Dimethoxy-4′-hydroxyacetophenone (acetosyringone)	Sigma-Aldrich	Cat#D134406
Tween® 20	Sigma-Aldrich	Cat#P9416
Triton™ X-100	Sigma-Aldrich	Cat#X100
Wizard® SV Gel and PCR Clean-Up System	Promega	Cat#A9281
Wizard® Plus SV Minipreps DNA Purification System	Promega	Cat#A1340
Critical commercial assays/components		
Gateway™ BP Clonase™ II Enzyme mix	Thermo Fisher Scientific	Cat#11789020
Gateway™ LR Clonase™ II Enzyme mix	Thermo Fisher Scientific	Cat#11791100
Gateway™ pDONR™207 Vector	Invitrogen	N/A
PrimeStar® Max DNA polymerase	Takara Bio	Cat#R045A
Phire Plant direct PCR kit	Thermo Fisher Scientific	Cat#F130WH
GoTaq® DNA polymerase	Promega	Cat#M3001
Nucleospin RNA Plus kit	Macherey-Nagel	Cat#740984
Turbo DNA-free	Invitrogen	Cat#AM1907
Transcriptor Reverse Transcriptase	Roche	Cat#3531287001
Takyon No ROX SYBR MasterMix blue dTTP	Eurogentech	Cat#UF-NSMT-B0701
Light Cycler 480 SYBR Green I Master	Roche Diagnostics	Cat#04887352001
PageRuler™ Prestained Protein Ladder, 10 to 180 kDa	Thermo Fisher Scientific	Cat#26617
4-15% Mini-PROTEAN® TGX™ Gels	Bio-Rad	Cat#4561083
4-15% Mini-PROTEAN® TGX™ Gels	Bio-Rad	Cat#4561086
Clarity™ Western ECL substrate	Bio-Rad	Cat#1705060
Clarity™ Max Western ECL substrate	Bio-Rad	Cat#1705062
Deposited data		
Raw and deposited data (Mendeley)	This paper	Reserved Mendeley Data: https://doi.org/10.17632/h869c2brt7.1 https://data.mendeley.com/preview/h869c2brt7?a=fb88da55-9321-4e7a-8d10-65802b5b016e

(*Continued on next page*)

Continued

REAGENT or RESOURCE	SOURCE	IDENTIFIER
Essential equipments		
Climatic chambers Memmert	Memmert	Cat#ICP110
Tissue Lyser MM 400 grinder	Retsch	Cat#20.745.0001
ChemiDoc™ imaging system	Bio-Rad	N/A
CFX Opus 384 Real-Time PCR	Bio-Rad	N/A
NanoDrop™ Lite	Thermo Fischer Scientific	Cat#ND-LITE
Gene Pulser Xcell Electroporation Systems	Bio-Rad	Cat#1652660
Experimental models: Organisms/strains		
E. coli DH5α		N/A
A. tumefaciens GV3101		N/A
Pseudomonas fluorescens Pf0-1		N/A
Nicotiana benthamiana		N/A
Arabidopsis thaliana Col-0		N/A
Arabidopsis thaliana Ag-0		N/A
Transgenic lines used in this study are listed in Table S1		N/A
Recombinant DNA		
Plasmids used in this study are listed in Table S2		N/A
Oligonucleotides		
Primers used in this study are listed in Table S3		N/A
Softwares		
R studio	On-line	https://www.r-project.org/
Geneious 11.1.4	Dotmatics	https://www.geneious.com/

EXPERIMENTAL MODEL AND STUDY PARTICIPANT DETAILS

Bacterial strains and growth conditions

Plasmids used in this study to transform *Agrobacterium tumefaciens* for plant transformation are listed in Table S2. *A. tumefaciens* strains were grown in liquid YEB medium (yeast extract 10 g/L, peptone 10 g/L, NaCl 5 g/L, pH7.0) supplemented with adequate antibiotics for 16 h at 28°C under shaking.

Pf0-1 strains were grown at 28°C on King's B agar medium (Peptone 20 g/L, Glycerol 10 g/L, K_2HPO_4 1.5 g/L, $MgSO_4.7H_2O$ 1.5 g/L, pH7.2) supplemented with adequate antibiotics overnight.

Plant material and growth conditions

Arabidopsis thaliana lines used in this study are listed in Table S1. Arabidopsis seeds were sown on MS media supplemented with antibiotics when needed, for transgenic lines selection. After 24h vernalization, MS plates were transferred in growth chambers under 16h photoperiod, 21°C conditions for eight to ten days. For seedling assays, eight to ten day-old seedlings were transferred to regulated climatic chambers (Memmert) set at 21°C or 30°C, under 8h photoperiod, after Dexamethasone treatment (see method details in Dex-induction section below). For adult plant Dex assays, eight day-old seedlings were transferred on soil pots (Jiffy) and grown for two to three weeks in growth chambers under 8h photoperiod conditions at 21°C, and transferred to climatic chambers (Memmert) set at 21°C or 30°C, under 8h photoperiod, after treatment (Dexamethasone and/or flg22, see details in Dex-induction section below). For *pADR1-L2:ADR1-L2^{DV}-HA* and *pNRG1.1:NRG1.1^{DV}-HA*, seeds were germinated on MS media, seven day-old seedlings were acclimated for approximately three days on soil pots at 21°C, then transferred and grown for two weeks in climatic chambers set at 21°C or 30°C.

METHOD DETAILS

Plasmid constructions

All plasmid constructs used for Arabidopsis stable transformation were generated by Gateway cloning (GWY, Invitrogen). PCR products flanked by attB sites were recombined into pDONR207 (Invitrogen) and then into dexamethasone-inducible pOpOff2-derived destination vectors pDex:GWY-FSBP, pDex:GWY-YFPv or pDex:GWY-MiniTurbo-3Flag.[44,63] Generation of pDex:GWY-FSBP

was previously described in.[44] The FSBP tag consists of a triple FLAG epitope (F) fused with a streptavidin-binding peptide (SBP).[44] pDex:GWY-YFPv or pDex:GWY-MiniTurbo-3Flag were modified from pOpOff2(Kan) GWY vector, which was kindly provided by Chris Helliwell (CSIRO, Canberra). This vector was lacking the hairpin GWY cassette (as described in[64]) and instead contained a simple GWY cassette but no terminator. Hence, a PCR fragment containing either the DNA sequence of the yellow fluorescent protein venus (YFPv)[65] or the MiniTurbo[66] with an in-frame triple FLAG epitope sequence, followed by the 35s terminator sequence, flanked with *KpnI*/*PmeI* restriction sites, were used to build pDex:GWY-YFPv or pDex:GWY-MiniTurbo-3Flag by restriction/ligation using pOpOff2(Kan)-GWY as the vector backbone. All plasmids and constructs were verified by sequencing. All plasmids, constructs and primers used in this study are listed in Tables S2 and S3.

Plant transformation and transgenic lines screening

Arabidopsis Col-0, and mutants in Col-0 background (*eds1-2*[67] or *RNL* mutants[21]), were transformed by floral-spraying or floral-dipping using *Agrobacterium tumefaciens* strains carrying *pDex:TIRs*, *pDex:TNLs* or *pDex:NRG1* constructs. Primary transformants were selected on MS media supplemented with hygromycin (50 μg/mL) and were individually PCR genotyped to verify the presence of the transgene or mutations in *RNLs* by using Thermo Scientific Phire plant direct PCR kit as previously described.[44] Primers used for PCR genotyping are listed in Table S3. Western-blot analyses were further performed on F2 progenies to verify protein accumulation of TIR or TNL constructs, 24h after dexamethasone induction of 8 day-old seedlings. *pADR1:ADR1-L2^{DV}-HA* line[50] and *pNRG1.1:NRG1.1^{DV}-HA* line[34] were kindly provided by Dr F. El Kasmi. All transgenic lines used in this study are listed in Table S1. For dry weight measurement, plants were individually harvested, dried in paper pockets at 37°C and weighed 3 days after.

Cell death assays upon dexamethasone induction and/or flg22 treatment

For seedling assays, seven to ten day-old seedlings were transferred on MS media plates supplemented with Dexamethasone (10μM) or DMSO (equivalent volume as Dexamethasone) and transferred to regulated climatic chambers (Memmert) set at 21°C or 30°C, under 8h photoperiod.

For adult plants assays, 8 day-old seedlings were transferred on soil pots (Jiffy) and grown for two to three weeks in a growth chamber under 8h photoperiod conditions at 22°C. Three to five leaves of three to five week-old plants were infiltrated with a needle-less syringe-with solutions containing 20 μM Dexamethasone or mock solution (equivalent volume of DMSO as Dexamethasone), a combination of flg22 peptide (100nM) and DMSO; or a combination of 20 μM Dexamethasone and 100nM flg22 solutions. For temperature assays, plants were transferred to regulated climatic chambers (Memmert) set at 21°C or 30°C, under 8h photoperiod upon Dex treatment. The apparition of cell death symptoms was monitored every day.

Cell death assays upon Pf0-1 infiltration

Three to four week-old plants were moved to climatic chambers (Memmert) set at 21°C or 30°C, under 8h photoperiod, for acclimation 48h prior Pf0-1 infiltration.

Pf0-1 strains were streaked on King's B agar plates containing appropriate antibiotics (tetracycline 10 μg/mL, chloramphenicol 30 μg/mL for empty Pf0-1 strain, additional gentamicin 15 μg/mL was added for Pf0-1 carrying *HopBA1*) and grown O/N at 28°C. Bacteria were resuspended in 10 mM $MgCl_2$ and bacterial density was adjusted to OD_{600nm} = 0.2.

Bacterial suspensions were then infiltrated in plant leaves with 1 mL needleless syringe and placed back in climatic chambers (21°C or 30°C). Plant material for RT-qPCR or WB analyses was collected 24h after infiltration on four different plants and eight different leaves (eight 4mm^2 discs). Cell death symptoms were scored 3 days after infiltration. Pf0-1 HopBA1 strain[48] was kindly provided by Prof. P. Schulze-Lefert (Max Planck Institute for Plant Breeding Research, Cologne).

Immunoblot analyses

For seedling assays, total protein extraction was performed on 10 eight day-old seedlings collected at different time points after Dexamethasone treatment. For adult plant assays, three or five 6mm leaf discs were harvested from three to five different plants per line carrying *pDex:RPS4^{TIR}* or *pDex:L6^{TIR}*, or lines carrying *pDex:RPS4* or *pDex:L6MHV*, respectively, 24h and 48h after treatment. For ADR1-L2^{DV}-HA detection, 7 leaf discs (diameter 1cm) were collected from 3 week-old plants grown at 21°C or 30°C. Plant material expressing TIR domains were ground and directly resuspended in 100μL of loading Laemmli buffer. Plant material expressing TNLs or RNLs were ground and resuspended in 100μL extraction buffer [150mM Tris-HCl pH7.5, 150mM NaCl, 1mM EDTA, NP-40 1%, Plant protease inhibitor cocktail (SIGMA) 1%, 10 mM DTT, 10 μM MG132], centrifuged for 5 min at 4°C to remove cell debris and 50μL of the supernatant was combined with 50μL loading Laemmli buffer (0.125 M Tris-HCl pH7.5, 4% SDS, 20% Glycerol, 0.2M DTT, 0.02% Bromophenol blue) for western-blot analysis. After denaturation at 95°C for 3 min, samples were then loaded on sodium dodecyl sulfate polyacrylamide gels for electrophoresis and transferred to nitrocellulose membranes which were blocked with 5% skimmed milk. Membranes were stained using Ponceau red staining to verify total protein loading. Membranes were further probed with anti-flag-horseradish peroxidase (HRP) (Sigma, SAB4200119) (dilution ratio: 1/5000), anti-c-myc-HRP (clone 9E10; Roche) (dilution ratio: 1/5000), or rabbit anti-EDS1 (kindly provided by J. E. Parker) (dilution ratio: 1/500) followed by incubation with a secondary goat anti-rabbit antibodies (Bio-Rad) conjugated to HRP (dilution ratio: 1/10000). Protein detection was performed using Bio-Rad Chemidoc Imaging system with the Bio-Rad Clarity Western ECL Substrate or Bio-Rad Clarity Max Western ECL Substrate.

RNA extraction and RT-qPCR analyses

Total RNA extraction was performed on 10 eight day-old seedlings or three 6mm leaf discs from three different four week-old plants at 24h and 48h after treatment. Total RNA was extracted using the Macherey Nagel Nucleospin RNA Plus kit following manufacturer's instruction. Total RNA was then subjected to DNAse treatment according to the Invitrogen Ambion TURBO DNA-free Kit instructions. 1μg total RNA was used for reverse transcriptase reactions. RT-qPCR reaction mix was prepared with SYBR green (Takyon No ROX SYBR 2X MasterMix blue dTTP) and run on Bio-Rad CFX Opus 384 Real-Time PCR instrument. Used primers are listed in Table S3.

QUANTIFICATION AND STATISTICAL ANALYSIS

For RT-qPCR data, mean ΔCt were calculated from three technical replicates from two to four biological replicates (as indicated in figure legends). *At1G13320* and *At5G15710* were used as internal control genes. Log2(2^{-}ΔCt) values were used to determine the significance of difference in gene expression between the different tested conditions, and were represented as boxplots using R studio. A two-ways ANOVA was used when the distribution of the data fitted assumptions of normality and homogeneity of variances, and was followed by a post-hoc pairwise comparison Tukey test.